Role for Myosin II in Regulating Positioning of *Salmonella*-Containing Vacuoles and Intracellular Replication[▽]

Julie A. Wasylnka,[1] Malina A. Bakowski,[1,2][¶] Jason Szeto,[1][¶] Maikke B. Ohlson,[5] William S. Trimble,[1,4] Samuel I. Miller,[5,6,7] and John H. Brumell[1,2,3]*

Cell Biology Program, Hospital for Sick Children, Toronto, Ontario M5G 1X8, Canada[1]; Department of Molecular Genetics,[2] Institute of Medical Science,[3] and Department of Biochemistry,[4] University of Toronto, Toronto, Ontario M5S 1A8, Canada; and Departments of Microbiology,[5] Genome Sciences,[6] and Medicine,[7] University of Washington, Seattle, Washington 98195-7710

Salmonella enterica serovar Typhimurium grows within host cells in a permissive compartment termed the *Salmonella*-containing vacuole (SCV). These bacteria use two distinct type III secretion systems (T3SS) to deliver virulence proteins (effectors) into cells. Effectors secreted by the *Salmonella* pathogenicity island 1 (SPI-1)-encoded T3SS mediate invasion and early SCV maturation steps, while those secreted by the SPI-2 T3SS affect the SCV at later stages postinfection. Some SPI-2 effectors modulate microtubule motor activity on the SCV. Here, we show that the actin-based motor myosin II also affects SCV dynamics during infection. Following invasion, myosin II is required for SCV positioning near the nucleus of host cells. Later, myosin II counteracts the activities of the SPI-2 effectors PipB2 and SseJ to maintain SCV positioning and stability, respectively. Myosin II activity was required for maximal bacterial growth in macrophages. Rho kinase activity was required for SCV positioning. The effector SopB, a known activator of Rho GTPases, was found to be required for SCV positioning, and transfection of cells with SopB was sufficient to induce myosin II phosphorylation. These studies reveal a novel role for myosin II in controlling SCV dynamics during infection and suggest that SopB activates myosin II.

The facultative intracellular pathogen *Salmonella enterica* serovar Typhimurium causes gastroenteritis in humans and a lethal systemic disease in certain strains of mice (74). These bacteria use two separate type III secretion systems (T3SS) to manipulate host cell machinery and direct their own entry into and replication in host cells. Invasion of epithelial cells is directed by the *Salmonella* pathogenicity island 1 (SPI-1)-encoded T3SS, a protein delivery system that translocates bacterial proteins (effectors) across the plasma membrane and into the host cell cytosol (22). These effectors interact with host signaling proteins, causing rearrangement of the underlying actin cytoskeleton (21). Cell surface ruffling drives uptake of the bacteria into *Salmonella*-containing vacuoles (SCVs) (23). Effectors of the SPI-1 T3SS also direct early maturation of the SCV (34, 64, 65, 67). Several hours after invasion, a second T3SS, encoded by SPI-2, delivers a separate set of effectors that aid in bacterial replication and survival in the host cell (30, 32, 62, 63).

The SCV is segregated from the normal host cell endocytic pathway, allowing the bacteria to replicate intracellularly and avoid lysosomal fusion (65). At early time points postinfection (p.i.; 0 to 60 min p.i.), the SCV migrates to the juxtanuclear region (28). Previous studies have suggested that this centripetal movement is mediated by microtubule-based motors (28). At later stages of infection, the SCV is maintained at the microtubule organizing center and associates with the Golgi apparatus (61). Positioning of the SCV is thought to be important for intracellular pathogenesis, as close apposition of SCV to the Golgi apparatus is associated with maximal intracellular bacterial growth (61).

Maintenance of SCV positioning at the juxtanuclear region is mediated by various SPI-2 T3SS effectors that manipulate microtubule motor activity at the SCV. SseF and SseG recruit dynein (1), while SifA recruits the host protein SKIP (SifA and kinesin-interacting protein) to uncouple kinesin (10). Another SPI-2 effector, PipB2, was shown to work antagonistically with SifA to promote kinesin accumulation on the SCV (29). Molecular motors also regulate vacuolar membrane integrity; inhibition of dynein or kinesin leads to destabilization of the SCV (25). In addition, kinesin activity is required for centrifugal extension of membranous *Salmonella*-induced filaments (Sifs) from the SCV (24, 28). Thus, serovar Typhimurium maintains a delicate balance of both plus- and minus-end-directed microtubule-based motors at the SCV to control its positioning and stability.

The SCV is associated with a network of actin, termed vacuole-associated actin polymerizations (VAP), that also extends along Sifs (12, 46, 48). VAP formation is largely dependent on the SPI-2 T3SS effector SteC; however, the mechanism by which it acts remains unclear (55). Depolymerization of VAP by cytochalasin D treatment causes serovar Typhimurium to escape from the SCV into the cytoplasm, a toxic environment in some cell types (8, 76). Despite the importance of VAP, a role for actin-based motors in serovar Typhimurium pathogenesis has not been examined to date.

Myosins are actin-based motors constituting a large super-

* Corresponding author. Mailing address: Cell Biology Program, Hospital for Sick Children, 555 University Avenue, Toronto, ON M5G 1X8, Canada. Phone: (416) 813-7654, ext. 3555. Fax: (416) 813-5028. E-mail: john.brumell@sickkids.ca.
¶ These authors contributed equally to the work in the paper.
▽ Published ahead of print on 14 April 2008.

family of more than 15 members (6). All myosins contain an ATPase motor domain which binds actin and drives movement, a neck domain that binds two light chains, and a tail domain that interacts with a specific cargo (47). The filament-forming class II myosin (conventional myosin II) is involved in muscle contraction (41) and cytokinesis (45), while unconventional nonmuscle myosin II participates in many diverse cellular functions, including phagocytosis, organelle transport, and signal transduction (47). Some pathogenic organisms use myosins to drive invasion and aid their movement within host cells. Cossart and colleagues have shown that uptake of *Listeria monocytogenes* requires myosin VIIA (66), while *Shigella flexneri* dissemination and murine leukemia virus infection were shown to be dependent upon myosin II (40, 59). In addition, several different myosins have been shown to be recruited to the phagocytic cup and localize to model phagosomes in macrophages (4, 16, 52, 72).

In this study, we asked whether nonmuscle myosin II plays a role in serovar Typhimurium pathogenesis. We demonstrate that myosin II maintains the SCV in a juxtanuclear position and maintains the integrity of this compartment during infection. Furthermore, we provide evidence that the SPI-1 effector SopB can regulate SCV positioning during early and late stages of infection through the activation of a Rho/Rho kinase (ROCK)/myosin II pathway. Thus, our findings reveal a central and previously unappreciated role for myosin II in controlling SCV dynamics within infected host cells.

MATERIALS AND METHODS

Cell culture. HeLa and RAW 264.7 cells were obtained from the ATCC and maintained in Dulbecco's modified Eagle's medium (HyClone) supplemented with 10% fetal bovine serum (Wisent) at 37°C with 5% CO_2 and without antibiotics. Cells were used between passages 5 and 30.

Strains, plasmids, and transfection. The serovar Typhimurium strains used in this study were CS401 (wild type [WT]) (49), CS800 ($\Delta ssaT$) (31), MBO87 ($\Delta sseJ$) (51), MBO107 ($\Delta sseJ$; complemented with a plasmid carrying *sseJ*) (51), and MBO106 ($\Delta sseJ$; complemented with a plasmid encoding a catalytically inactive mutant of SseJ [with mutations S151A, D247N, and H384N]) (51), which have all been described previously. MBO207 ($\Delta pipB2$) was generated in the CS401 background. WT serovar Typhimurium SL1344 (35) and isogenic mutants including M202 ($\Delta sopE$ $\Delta sopE2$ mutant) (70), $\Delta sopB$ (68), a $\Delta sopB$ mutant complemented with *sopB* (68), and a $\Delta sopB$ mutant complemented with a plasmid carrying the catalytically inactive (C462S) mutant of *sopB* (68) have all been described previously. Serovar Typhimurium SL1344/p*sifA-2HA* (12) was used for the SifA colocalization experiments.

Bacteria were grown in Luria-Bertani (LB) broth supplemented with streptomycin, carbenicillin, kanamycin (all at 50 µg/ml), or chloramphenicol (30 µg/ml) as required.

Plasmids used were pegfp-N1 (Clontech); pmrlc2-WT and pmrlc2-AA (19) (generously provided by G. Egea, University of Barcelona); psopB∆GFP (42); prhoA-Q63L, pCdc42-Q61L, and prhoG-Q61L (33) (generously provided by W. D. Heo and T. Meyer, Stanford University); and pDN-ROCK (44), pCAT-ROCK (2), and pMLC-DD (36) (generously provided by A. Kupas, University Health Network, Toronto, Ontario, Canada). Plasmids were transfected into cells 16 h before infections/immunostaining using Fugene 6 (Roche) or Gene Juice (Promega) transfection reagents according to manufacturers' instructions.

Bacterial infection of cultured cells. *Salmonella* infections were performed as previously described (69). Briefly, bacteria were grown for 16 h at 37°C with shaking and then subcultured (1:33) for 3 h in LB broth. Late-log-phase bacteria were used at a multiplicity of infection of approximately 300:1 to infect cells with a brief (10-min) exposure to bacteria. Drugs (from Sigma; see below) were added at 10 min p.i. and cells were fixed at 2 h p.i. or drugs were added at 2 h p.i. and cells were fixed at 8 h p.i. in 20 µM blebbistatin, 0.5 µg/ml cytochalasin D, 2 µg/ml nocodazole in 1% dimethyl sulfoxide (DMSO), 5 µM Y-27632 in 1% DMSO, or 2 nM calyculin A in 1% DMSO.

siRNA. To knock down expression of myosin IIA and ROCK I and ROCK II, small inhibitory RNAs (siRNAs) (Dharmacon) were used. HeLa cells were seeded into 24-well culture plates at 2.5×10^4 cells per well. The following day, cells were transfected using Oligofectamine (Invitrogen) with either control siRNA (pool of four nontargeting siRNAs [siCONTROL, D-001206-13-05; Dharmacon]) or siRNA directed against myosin IIA (siGENOME SMARTpool, M-007668-00; Dharmacon) or both ROCK I (5′-GAG GCT CAA GAC ATG CTT A-3′) and ROCK II (5′-GGC ATC GCA GAA GGT TTA T-3′) (Dharmacon). A concentration of 50 nM of total siRNA was used in each knockdown. Medium was changed 24 h after transfection, and HeLa cells were infected with serovar Typhimurium 48 h after transfection.

SCV position measurements. Intracellular SCV positions were determined by measuring the distances from lysosome-associated membrane protein-1-positive (LAMP-1$^+$) SCVs to the nearest edge of the nucleus (labeled by DAPI [4′,6′-diamidino-2-phenylindole]). Images of infected cells were acquired by epifluorescence microscopy. Measurements were determined using Openlab 3.1.7 software (Improvision). The distances from ≥100 LAMP-1$^+$ SCVs to the nucleus were measured for each time point. Average distances ± standard errors (SE) for three separate experiments were determined. Average cell surface areas were also determined by tracing cell outlines (>30 cells per time point or drug treatment for each of three separate experiments) imaged by epifluorescence or differential interference contrast microscopy and determining surface area by using Openlab software.

Immunofluorescence. Cells were fixed for 10 min at 37°C in phosphate-buffered saline (PBS), pH 7.2, containing 2.5% paraformaldehyde. Fixed cells were washed with PBS and then permeabilized/blocked in PBS–10% normal goat serum containing 0.2% saponin. For phospho-myosin II light chain (PP-MLC) staining, cells were washed for 10 min with PBS–100 mM glycine prior to permeabilization. Samples were incubated separately with primary and secondary antibodies diluted in the PBS–10% normal goat serum containing 0.2% saponin for 1 h each and then washed three times with PBS. Coverslips were mounted onto glass slides by using antifade mounting reagent (DakoCytomation) and were analyzed by using a Leica DMIRE2 epifluorescence microscope.

For confocal microscopy, cells were immunostained as described above and then analyzed on a spinning-disk confocal microscope. Confocal sections of 0.25 µm were acquired by using a Leica DMIRE2 inverted fluorescence microscope equipped with a Hamamatsu back-thinned electron multiplying charge-coupled-device camera and spinning-disk confocal scan head. Velocity 4 (Improvision) software was used to assemble confocal *z* sections into flattened projections and for movie construction. Image assembly was done using Adobe PhotoShop and Adobe Illustrator software.

Antibodies. Mouse anti-LAMP-1 H4A3 monoclonal antibody (used at a dilution of 1:50) developed by T. August was obtained from the Developmental Studies Hybridoma Lab under the auspices of the NICHD, National Institutes of Health Sciences, and maintained by the University of Iowa, Iowa City, IA. Bacteria were detected by using either anti-*Salmonella* group B rabbit polyclonal antibodies from Difco at 1:100 or a monoclonal anti-*Salmonella* antibody (BioDesign International) at 1:100. Actin was detected by using Alexa Fluor 568-conjugated phalloidin (Molecular Probes) at 1:50; rabbit polyclonal myosin IIA heavy chain antibodies from Covance were used at 1:200. Transfected cells were detected using either a monoclonal antibody to the myc epitope tag (1:50) (Covance), a polyclonal anti-green fluorescent protein (GFP) antibody (1:200) (Clontech), or a monoclonal anti-GFP antibody (1:200) (Invitrogen). Phospho-myosin II was detected with the rabbit Ser 18/Thr19 phospho-myosin II antibody from Cell Signaling (1:50 for immunofluorescence, 1:1,000 for Western blotting). Hemagglutinin (HA) was detected using the monoclonal HA.11 (Covance) at 1:100 for 4 h. A rabbit polyclonal kinesin antibody against the kinesin heavy chain was used at 1:500 (PCP42; a gift from Ron Vale, University of California). The following secondary antibodies were used at 1:200: Alexa Fluor 568-conjugated goat anti-rabbit immunoglobulin G (IgG), Alexa Fluor 350-conjugated goat anti-rabbit IgG, Alexa Fluor 488-conjugated goat anti-rabbit IgG, Alexa Fluor 488-conjugated goat anti-rat IgG, Alexa Fluor 488-conjugated goat anti-mouse IgG, and Alexa Fluor 568-conjugated goat anti-mouse IgG (all from Molecular Probes). For some experiments, mouse anti-LAMP-1 H4A3 was conjugated to Alexa Fluor 568 by using the Zenon Alexa Fluor 568 mouse IgG labeling kit (Molecular Probes). To detect myosin II during Western blotting with siRNA-treated cell extracts, rabbit anti-nonmuscle myosin heavy chain (BT-561) (Biomedical Technologies Inc.), which detects both myosin IIA and IIB isoforms, was used at 1:1,000. To detect ROCK II, rabbit anti-ROKα/ROCK II (clone A9W4) (Upstate) was used at 1:1,000.

PP-MLC Western blotting. HeLa cells were seeded into 24-well culture plates at 2.5×10^4 cells per well. The following day, cells were transfected with Lipofectamine 2000 (Invitrogen) with indicated constructs. Cells were washed

with cold PBS (without magnesium and without calcium), and cell lysates were collected 17 h following transfection.

Statistics. For all experiments, average values and standard deviations (SD)/SE for three experiments were determined, and ≥100 bacteria/SCVs/Sifs/cells were counted for each treatment/sample within an experiment. Depending on the nature of the experiment, statistical analyses were performed using either a two-tailed unpaired *t* test or a one-way analysis of variance (ANOVA) (Prism 4 software). *P* values of <0.05 were considered significant.

RESULTS

Myosin II inhibition affects SCV stability and growth in host cells. Disruption of the host cell actin cytoskeleton during serovar Typhimurium infection causes destabilization of the SCV, resulting in bacterial escape into the cytosol (46). To investigate the potential effect of actin motors on SCV stability, we used blebbistatin to inhibit the nonmuscle myosin II in HeLa cells. In control cells, ~78% of the WT bacteria were present in SCVs at 8 h p.i., as determined by colocalization with the SCV marker LAMP-1 (Fig. 1A). In contrast, blebbistatin-treated cells had only 58% of bacteria in SCVs, suggesting that myosin II regulates SCV stability. We saw, besides decreased SCV stability, an increase in the number of intracellular bacteria in blebbistatin-treated cells by 10 h p.i. (Fig. 1B), consistent with the observation that the cytosol of HeLa cells permits serovar Typhimurium replication (8, 13). We noted that myosin II inhibition with blebbistatin did not affect the efficiency of bacterial entry into cells (data not shown). In HeLa cells infected with the isogenic (SPI-2-deficient) ΔssaT mutant (31), myosin II inhibition had no effect on SCV stability; the numbers of bacteria in SCVs were ~75% in control and drug-treated cells (Fig. 1A). Hence myosin II inhibition leads to destabilization of SCVs in a manner dependent on the SPI-2 T3SS.

Growth of serovar Typhimurium in vivo is correlated with the ability to replicate in macrophages (20), so we tested whether myosin inhibition in macrophages affects SCV stability and/or replication. RAW 264.7 cells were infected for 2 h with WT or ΔssaT serovar Typhimurium, and DMSO or blebbistatin was added to the media for an additional 8 h. In contrast to the case for HeLa cells, blebbistatin treatment of RAW 264.7 cells did not affect SCV stability (Fig. 1C). However, at 10 h p.i., ~39% of control cells contained >15 bacteria, while the percentage of such blebbistatin-treated cells was ~15% (Fig. 1D). Decreased bacterial growth without a decrease in SCV stability may occur if myosin inhibition affects macrophage trafficking. Since the macrophage cytosol is cytotoxic for serovar Typhimurium (8), LAMP-1-negative bacteria may also have been degraded by 10 h p.i.

Myosin II counteracts the SCV-destabilizing activity of SseJ. SseJ is a SPI-2 effector with deacylase activity (51) and antagonizes the SCV-stabilizing effect of SifA (60). To see if SseJ plays a role in bacterial escape from SCVs in the absence of myosin II activity, we infected HeLa cells for 8 h with WT, ΔsseJ, or ΔsseJ bacteria complemented with plasmids encoding WT SseJ or a catalytically inactive mutant of SseJ (51) in the presence of DMSO or blebbistatin. In contrast to the SCV stability of the WT strain, SCV stability of the ΔsseJ strain was unaffected by blebbistatin, with ~75% LAMP-1+ bacteria in control and drug-treated HeLa cells (Fig. 1A). Complementation of ΔsseJ bacteria with WT psseJ plasmid restored the

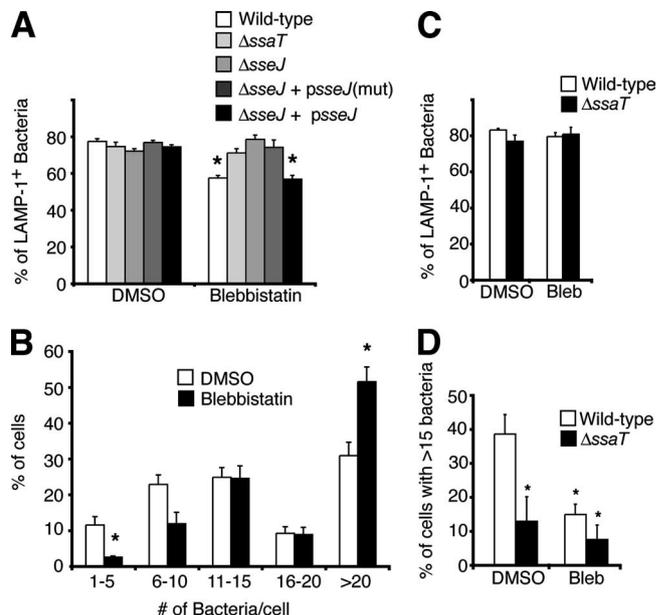

FIG. 1. Myosin II regulates intracellular growth of serovar Typhimurium. (A) Percent LAMP-1+ bacteria 8 h p.i. in HeLa cells infected with indicated serovar Typhimurium strains. Blebbistatin was added at 2 h p.i. as indicated. mut, encoding a mutated form of SseJ; ∗, significantly different from the respective DMSO-treated control (*P* < 0.05; two-tailed, unpaired *t* test). (B) Numbers of bacteria in 100 cells from samples described above for panel A were counted. ∗, significantly different from the respective DMSO-treated control (*P* < 0.05; two-tailed, unpaired *t* test). (C) RAW 264.7 cells were infected with WT or ΔssaT serovar Typhimurium, treated, immunostained, and counted as described above for panel A. (D) Numbers of bacteria in cells described for panel C were counted. Percentages of cells containing >15 bacteria are shown in all cases. Averages ± SE are shown in all cases. ∗, significantly different from the WT DMSO-treated control (*P* < 0.05), as determined by one-way ANOVA and Newman-Keuls post hoc analysis. Bleb, blebbistatin.

destabilizing effect of blebbistatin, unlike the expression of a catalytically inactive SseJ mutant (Fig. 1A). Hence, the deacylase activity of SseJ is required to destabilize the SCV in the absence of myosin II activity.

Myosin II mediates juxtanuclear positioning of the SCV following invasion. Recent studies have suggested that, in addition to SCV stability, the movement of the SCV to the juxtanuclear region is dependent on microtubule motors (25, 28). Therefore, we asked whether the actin cytoskeleton also plays a role in this positioning. HeLa cells were infected with WT serovar Typhimurium and then immediately (10 min p.i.) treated with the actin-depolymerizing agent cytochalasin D. At 2 h p.i., cells were fixed and immunostained for bacteria and LAMP-1. To measure SCV positioning, the distances from intracellular bacteria within vacuoles (LAMP-1+) to the closest nuclear edge were determined, as performed in other studies (1, 10, 11, 28, 29), and these values were averaged for each experiment (see Materials and Methods). For control (DMSO-treated) cells, we observed that SCVs were 2.7 ± 0.5 μm from the nucleus (Fig. 2A and B). We were concerned that cytochalasin D treatment would affect cell morphology and hence influence the positions of SCVs relative to the nucleus. Therefore, we measured the surface area of the infected cell at the
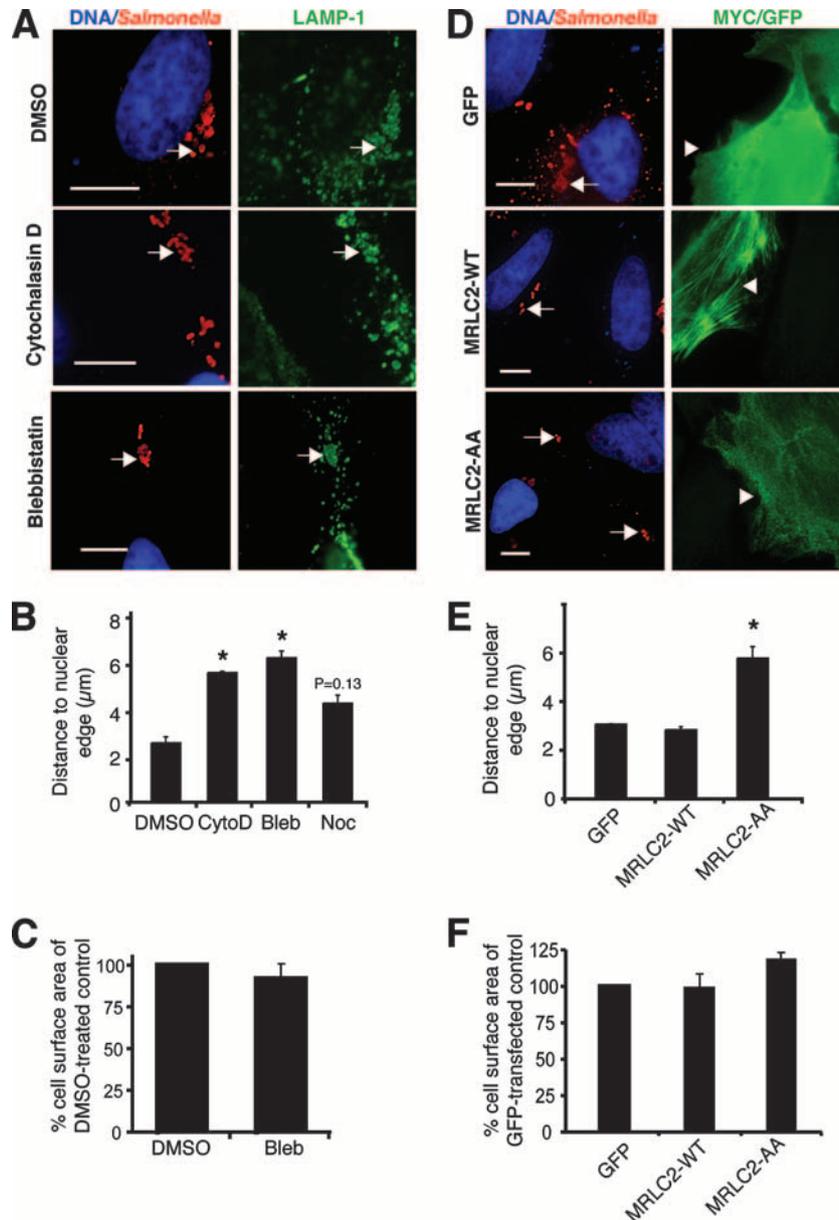
FIG. 2. Myosin II regulates positioning of the SCV during early stages of infection. CytoD, cytochalasin D; Bleb, blebbistatin; Noc, nocodazole. (A) Positions of serovar Typhimurium bacteria (red) 2 h p.i. in HeLa cells treated with the indicated drugs. LAMP-1 is shown in green, and nuclei are shown in blue. Arrows indicate LAMP-1$^+$ bacteria. Bars, 10 μm. (B) Measurements of LAMP-1$^+$ bacteria to the closest nuclear edge in drug-treated cells. ∗, significantly different from DMSO-treated control cells ($P < 0.05$) as determined by one-way ANOVA and Dunnett post hoc analysis. Averages ± SE are shown. (C) Comparison of the surface area of blebbistatin-treated HeLa cells in relation to DMSO-treated control cells. No significant differences were observed, as determined by a two-tailed, unpaired t test. Averages ± SE are shown. (D) Positions of serovar Typhimurium bacteria (red) 2 h p.i. in cells expressing GFP, MRLC2-WT, or MRLC2-AA (green). Transfected cells are indicated by arrowheads, and bacteria are indicated by arrows. Size bars, 10 μm. (E) Measurements of LAMP-1$^+$ bacteria to the closest nuclear edge in GFP-, MRLC2-WT-, and MRLC2-AA-transfected cells. Averages ± SE are shown. ∗, significantly different from GFP- and MRLC2-WT-transfected cells ($P < 0.05$) as determined by one-way ANOVA and Dunnett post hoc analysis. (F) Comparison of the surface areas of transfected cells from panel D. No significant differences were observed, as determined by one-way ANOVA and Dunnett post hoc analysis. Averages ± SE are shown.

interface with the glass coverslip by using Openlab software (see Materials and Methods). Even though use of cytochalasin D resulted in some shrinkage of HeLa cells (as determined by a drop in surface area [data not shown]), SCVs in these cells were significantly farther from the nucleus than the SCVs in the untreated controls were (Fig. 2B). This suggested that actin is important for SCV positioning.

Next, we treated HeLa cells with the myosin II inhibitor blebbistatin, as described above. After 2 h of treatment, SCVs of the blebbistatin-treated cells were significantly farther from the nucleus than those of the controls were (Fig. 2A and B). Treatment with blebbistatin did not induce significant changes in infected host cell surface areas in comparison to those of untreated, infected controls (Fig. 2C); hence, the effects of the
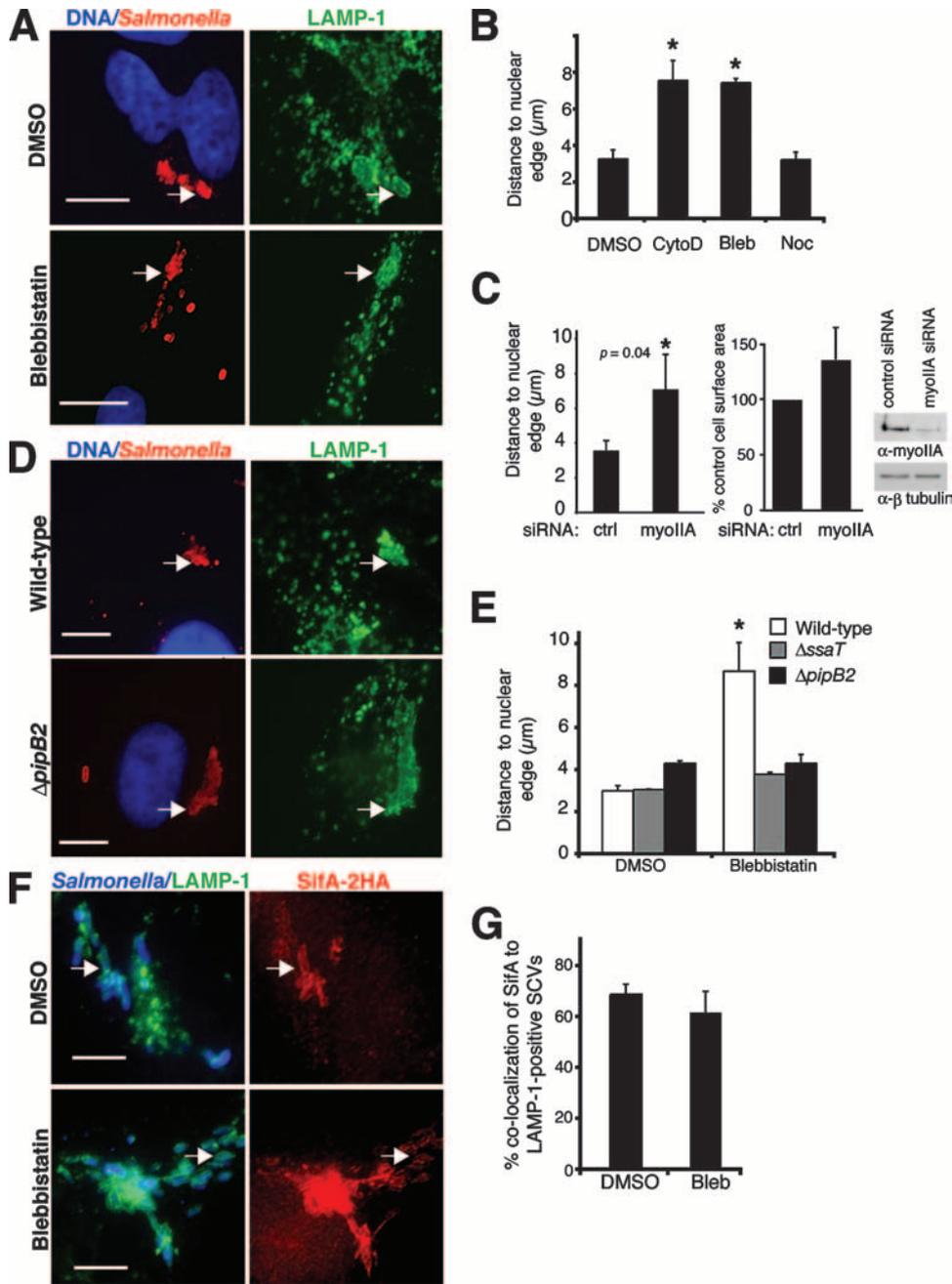
FIG. 3. Myosin II regulates positioning of the SCV during later stages of infection. (A) Positions of serovar Typhimurium bacteria (red) 8 h p.i. in HeLa cells treated with the indicated drugs. LAMP-1 is shown in green, and nuclei are shown in blue. Arrows indicate LAMP-1$^+$ bacteria. (B) Measurements of LAMP-1$^+$ bacteria to the closest nuclear edge in drug-treated cells. *, significantly different from DMSO-treated controls ($P < 0.01$), as determined by one-way ANOVA and Dunnett post hoc analysis. Averages ± SE are shown. CytoD, cytochalasin D; Bleb, blebbistatin; Noc, nocodazole. (C) Positions of serovar Typhimurium bacteria 8 h p.i. in cells treated with control (ctrl) or myosin IIA (myoIIA) siRNA. Averages ± SD are shown. *, significantly different from DMSO-treated controls ($P < 0.05$), as determined by a two-tailed, unpaired t test. A Western blot showing knockdown of nonmuscle myosin IIA in HeLa cells treated with myosin IIA siRNA is shown. (D) Positions of WT and Δ$pipB2$ serovar Typhimurium bacteria (red) 8 h p.i. in blebbistatin-treated cells. LAMP-1 is shown in green, and nuclei are shown in blue. Arrows indicate LAMP-1$^+$ bacteria. (E) Measurements of LAMP-1$^+$ bacteria to the closest nuclear edge in drug-treated cells. (F) WT serovar Typhimurium expressing a p$sifA-2HA$ plasmid (blue) 8 h p.i. in cells treated with the indicated drugs. SifA is shown in red (HA), and LAMP-1 is shown in green. Arrows indicate colocalization of LAMP-1$^+$ bacteria and SifA. (G) Colocalization of LAMP-1$^+$ bacteria with SifA (HA) was quantified. For panels E and G, averages ± SE are shown. *, significantly different from the respective DMSO-treated controls ($P < 0.05$), as determined by a two-tailed, unpaired t test. Bars, 10 μm.

drug on SCV positioning were not due to grossly disrupted cell morphology. Blebbistatin treatment did not affect Golgi apparatus or lysosome distribution, nor did it affect the dynamics of Rab5 (early endosomal), Rab11 (recycling endosome), or

LAMP-1 acquisition on the SCV (data not shown), indicating that the effect of blebbistatin on SCV localization was not due to altered maturation of this compartment. SCVs in nocodazole-treated cells were farther from the nucleus than those in

controls were, but the difference was not statistically significant ($P = 0.13$) (Fig. 2B). The average cell surface area of nocodazole-treated cells did not differ significantly from the average cell surface area of DMSO-treated controls (data not shown).

Next, we inhibited myosin II by using a dominant negative myc-tagged MLC construct that cannot be phosphorylated (MRLC2-AA) and is therefore inactive (19). As controls, HeLa cells were transfected with GFP or a myc-tagged WT myosin regulatory light chain construct (MRLC2-WT) (19). Transfected cells were infected for 2 h with WT serovar Typhimurium, fixed, and immunostained, and the distances from SCVs to the nucleus in transfected cells were measured (Fig. 2D and E). Bacteria were on average 3.1 ± 0.02 μm from the nucleus in GFP-transfected cells and 2.8 ± 0.13 μm from the nucleus in MRLC2-WT-transfected cells (Fig. 2E). In contrast, SCVs in MRLC2-AA-transfected cells were significantly farther from the nucleus (5.8 ± 0.5 μm) (Fig. 2E). Measurements of average cell surface areas did not reveal any significant differences between control GFP-transfected cells and those transfected with MRLC2-WT or MRLC2-AA (Fig. 2F). These findings suggest that myosin II plays a major role in regulating movement of the SCV from the host cell periphery to the perinuclear region during early infection.

Myosin II regulates positioning of the SCV during late infection. During late stages of infection (8 to 14 h p.i.), SCVs are maintained at a perinuclear position through actions of SPI-2 T3SS effectors that modulate microtubule motor activity (1, 10, 25, 29, 58). To investigate a role for actin in SCV positioning at later stages of infection, we treated HeLa cells with cytochalasin D at 2 h p.i. (after the bacteria had moved to the perinuclear region) and incubated them for an additional 6 h. Despite some host cell shrinkage in the presence of cytochalasin D, SCVs in these drug-treated cells were still farther from the nuclear edge (7.6 ± 1.1 μm) than were SCVs in control cells (3.3 ± 0.5 μm) (Fig. 3B). Blebbistatin treatment also led to a peripheral dispersion of SCVs at this time point (Fig. 3A and B). The average cell surface area of infected blebbistatin-treated cells did not differ significantly from that of the infected DMSO-treated controls (data not shown). Nocodazole treatment had no effect on SCV positioning (Fig. 3B).

To further confirm the role of myosin II in SCV positioning, we used siRNA to knock down myosin IIA expression in HeLa cells prior to invasion with WT serovar Typhimurium, since myosin IIA is the dominant isoform of myosin II in HeLa cells (77). As shown in Fig. 3C, treatment of cells with siRNA against myosin IIA resulted in an increase in the average distance between SCVs and the nucleus at 8 h p.i. in comparison to the value for the cells treated with control siRNA. There was no significant difference in average cell surface area between infected control siRNA- and myosin IIA siRNA-treated cells (Fig. 3C). Western blotting using antibody directed against both myosins IIA and IIB verified the knockdown of myosin IIA in HeLa cells treated with myosin IIA siRNA, with densitometric analysis indicating a >80% knockdown in comparison to control cells (Fig. 3C). Together, these results demonstrate that myosin II regulates SCV positioning during both early and late stages of infection.

Myosin II counteracts the kinesin-recruiting effector PipB2. It was not immediately obvious why myosin II inhibition caused centrifugal displacement of SCVs at 8 h p.i. We hy-
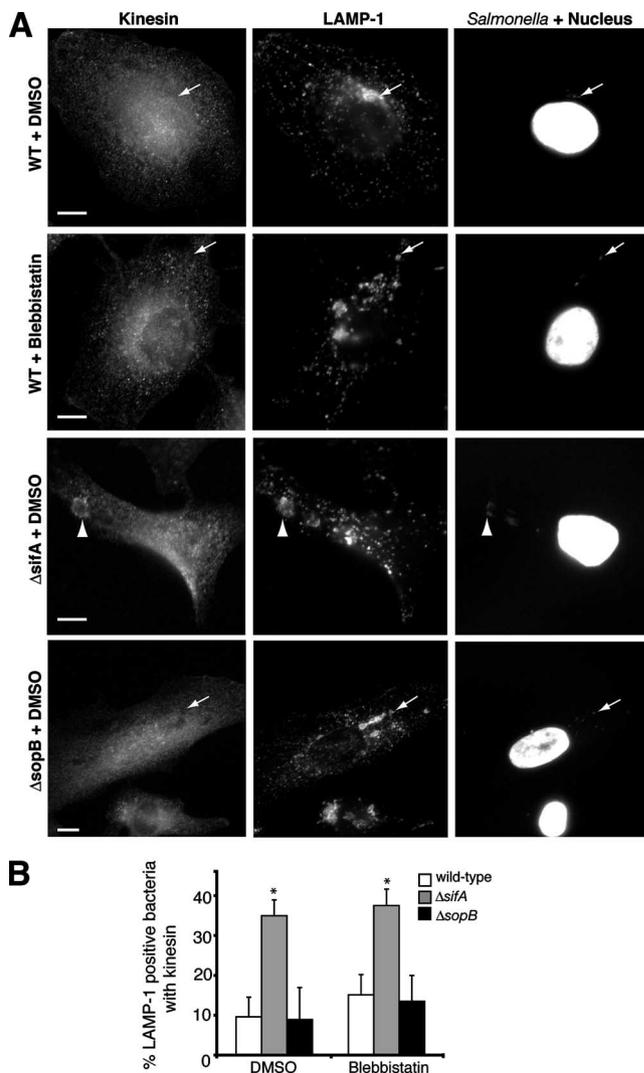
FIG. 4. Inhibition of myosin II or loss of SopB does not affect kinesin accumulation on the SCV. (A) HeLa cells were infected with WT serovar Typhimurium or isogenic Δ*sopB* or Δ*sifA* strains for 8 h. Cells were fixed and immunostained for bacteria, LAMP-1, and kinesin and analyzed by immunofluorescence microscopy. Representative images of cells infected with WT (upper two rows), Δ*sifA* (middle rows), or Δ*sopB* (lower rows) strains are shown. Bars, 10 μm. Arrows indicate LAMP-1-positive bacteria in SCVs that do not colocalize with kinesin, and arrowheads indicate LAMP-1-positive bacteria in an SCV that do colocalize with kinesin. (B) Samples shown in panel A were analyzed by counting the number of LAMP-1-positive bacteria that also colocalized with kinesin. The averages ± SE of three experiments are shown. At least 100 LAMP-1-positive bacteria were measured for each treatment. ∗, significantly different from DMSO-treated controls ($P < 0.05$), as determined by one-way ANOVA and Dunnett post hoc analysis.

pothesized that microtubule motors, such as kinesin, might mediate centrifugal SCV displacement in the absence of myosin II activity and that SPI-2 effectors may promote this. To test this, HeLa cells were infected with WT or isogenic Δ*ssaT* (SPI-2 T3SS-defective) serovar Typhimurium strains for 2 h, then blebbistatin was added to the media, and this was followed by an additional 6-h incubation. As expected, WT bacteria were peripherally displaced from the nucleus in the pres-
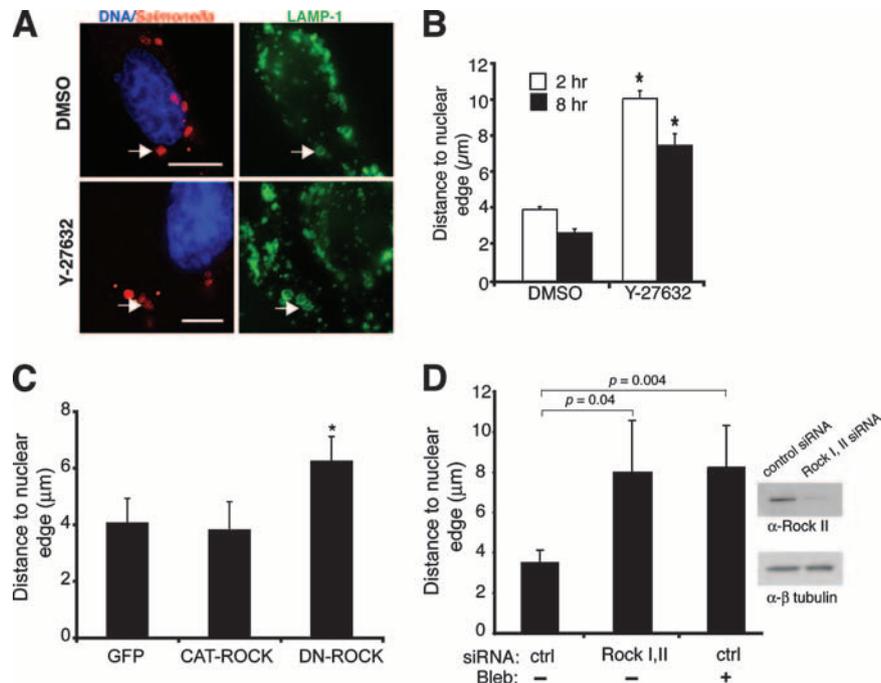
FIG. 5. Inhibition of ROCK affects SCV positioning. (A) HeLa cells were infected with serovar Typhimurium for 10 min, and then DMSO or the ROCK inhibitor Y-27632 was added to the medium until 2 h p.i. For late-infection experiments, cells were infected for 2 h, and then DMSO or Y-27632 was added to the medium for an additional 6 h. Cells were fixed and immunostained for *Salmonella* and LAMP-1 and analyzed by immunofluorescence microscopy. Representative images of cells treated with DMSO or Y-27632 are shown. Arrows indicate LAMP-1-positive bacteria. Bars, 10 μm. (B) Samples shown in panel A were analyzed by measuring the distance from the LAMP-1$^+$ bacteria to the closest nuclear edge. Averages ± SE are shown. *, significantly different from the respective DMSO-treated controls ($P < 0.05$), as determined by a two-tailed, unpaired *t* test. (C) Cells were transfected with pegfp, pCAT-ROCK, or pDN-ROCK and infected with WT serovar Typhimurium for 8 h. Cells were fixed and immunostained for *Salmonella* and LAMP-1, and the cells were stained with DAPI as well. The distances from LAMP-1$^+$ bacteria to the closest nuclear edge were determined. Averages ± SD are shown. Asterisks indicate values that are significantly different ($P < 0.05$) from those of control GFP-transfected cells, as determined by one-way ANOVA and Dunnett post hoc analysis. (D) Cells treated with either control siRNA (ctrl) or siRNA directed against ROCK I and II (Rock I,II) were infected with WT serovar Typhimurium for 8 h. Blebbistatin (Bleb) was also added at 2 h p.i. as indicated. Cells were fixed and immunostained as described above. The distances from LAMP-1$^+$ bacteria to the closest nuclear edge were determined. Averages ± SD are shown. A Western blot demonstrating knockdown of ROCK II in HeLa cells that received ROCK I and II siRNA is shown.

ence of the drug (Fig. 3D and E). However, Δ*ssaT* bacteria were not affected by blebbistatin treatment and remained perinuclear (Fig. 3E). This suggested that SPI-2 effector(s) would mediate outward displacement of the SCV in the absence of myosin II activity.

In the absence of SifA, PipB2 promotes accumulation of kinesin on the SCV, leading to its centrifugal displacement (29). Hence, we hypothesized that PipB2 mediates centrifugal SCV displacement in the absence of myosin II activity as well. Compared to its isogenic WT strain, the Δ*pipB2* strain maintained a juxtanuclear position at 8 h p.i. in the presence of blebbistatin (Fig. 3D and E). These findings show that PipB2 promotes outward movement of the SCV when myosin II activity is inhibited.

SCV positioning is also regulated by SifA, which interacts with the host protein SKIP to uncouple kinesin from the SCV (10). In the absence of *sifA*, SCVs accumulate kinesin and are situated away from the nucleus (Fig. 4A, third row) (10), in contrast to the juxtanuclear positioning of WT SCVs at 8 h p.i. (Fig. 4A, top row). To determine if myosin inhibition affects SifA and kinesin recruitment, we infected HeLa cells with WT serovar Typhimurium expressing p*sifA-2HA* and treated cells with blebbistatin. Neither SifA colocalization with SCVs (Fig.

3F and G) nor kinesin recruitment to WT SCVs (Fig. 4A, second row, and B) was affected in blebbistatin-treated cells. Therefore, inhibiting myosin function is sufficient to cause centrifugal SCV displacement without increasing kinesin levels on SCVs.

ROCK is required for normal SCV positioning. Activation of myosin II is regulated by phosphorylation of MLC by several kinases, including ROCK (3, 75). ROCK also indirectly promotes MLC phosphorylation by inhibiting myosin II phosphatase, thus maintaining myosin II in its active state (78). Since serovar Typhimurium can modulate several members of the Rho family, including Cdc42, Rac, and RhoG (27, 54, 80), we attempted to determine a role for ROCK in myosin activation during serovar Typhimurium infection. HeLa cells were infected and treated with the ROCK inhibitor Y-27632 at 10 min p.i. After 2 h, internalized bacteria in the drug-treated cells were displaced farther from the nucleus than the bacteria in the controls were (Fig. 5A and B). ROCK inhibition also prevented the SCV from localizing to the perinuclear region at 8 h p.i. (Fig. 5B). Treatment of cells with Y-27632 did not grossly affect host cell morphology, as determined by comparing average cell surface areas of drug-treated and control cells (data not shown). Transfection of HeLa cells with a dominant

negative Rho-associated kinase construct (DN-ROCK) (44) also caused centrifugal displacement of SCVs, but transfection with a constitutively active ROCK II catalytic-domain construct (CAT-ROCK) (2) or GFP did not (Fig. 5C). Treatment of HeLa cells with siRNA specific to ROCK I and ROCK II also resulted in an increase in the average distance of SCVs from the nucleus at 8 h p.i. (Fig. 5D). Inhibition of ROCK I and II did not affect the average cell surface area of treated cells in comparison to that of cells receiving control siRNA (data not shown). Western blotting verified >85% knockdown of ROCK II in HeLa cells treated with ROCK I and ROCK II siRNA (Fig. 5D). Commercially available antibodies did not detect ROCK I in Western blotting of HeLa cell lysates, possibly due to its low expression in this cell type. Overall, these data show that a known activator of myosin II, namely, ROCK, is required for normal SCV positioning throughout infection.

SopB is required for maintaining SCV positioning. Our experiments suggested that SCV positioning might be regulated by members of the Rho GTPase family, acting via ROCK activation. The SPI-1 T3SS effectors SopE, SopE2, and SopB promote invasion by activating host cell Rho GTPases. SopE and SopE2 function as guanine nucleotide exchange factors that activate Cdc42 and Rac1 (27, 70), while SopB is a phosphoinositide phosphatase that activates Cdc42 and RhoG by an unknown mechanism(s) (54, 80). SopE/SopE2 are rapidly degraded following bacterial entry (39). Since SopB protein levels persist in the host cell for up to 12 h p.i. (17), we hypothesized that this protein may regulate SCV positioning. To test this idea, we infected HeLa cells with WT or $\Delta sopB$ serovar Typhimurium for up to 10 h and measured the distance from SCVs to the nucleus. For a positive control, cells were infected with a $\Delta sifA$ mutant, since SifA controls SCV positioning by uncoupling kinesin from the vacuole (10). At 10 h p.i., SCVs containing the $\Delta sopB$ and $\Delta sifA$ mutants were significantly farther from the nucleus than the WT bacteria were (Fig. 6A and B). Similar results were seen at 2, 4, and 8 h, suggesting that SopB controls SCV positioning throughout infection (data not shown). In contrast, cells infected with a $\Delta sopE \, \Delta sopE2$ double mutant strain showed no SCV positioning defects (data not shown). Complementation of the $\Delta sopB$ strain with a plasmid encoding WT SopB restored normal SCV positioning near the nucleus. However, a plasmid encoding SopB with a mutation in the conserved catalytic site (C462S) (43) did not complement the $\Delta sopB$ phenotype (Fig. 6B). myc-tagged SopB was localized to SCVs up to 10 h p.i. (Fig. 7A). This suggests that SopB acts through its phosphatase activity to regulate SCV positioning.

Recently, Brawn et al. showed that another SPI-1 effector, SipA, recruits SifA to the SCV (11). To see if SopB acts similarly, we infected cells with a WT strain with p*sifA-2HA* or a $\Delta sopB$ strain with p*sifA-2HA* for 8 h and immunostained for bacteria, HA, and LAMP-1. SifA colocalized with both the WT and $\Delta sopB$ mutant SCVs (Fig. 7B and C). Since SifA downregulates kinesin on the SCV (10), we also tested whether kinesin recruitment to the SCV was altered in $\Delta sopB$-infected HeLa cells. No kinesin recruitment to either WT or $\Delta sopB$ mutant SCVs was seen (Fig. 4A, first and fourth rows, and B). In contrast, up to 35% of the $\Delta sifA$ mutant SCVs colocalized with kinesin (Fig. 4A, third row, and B). These data suggest
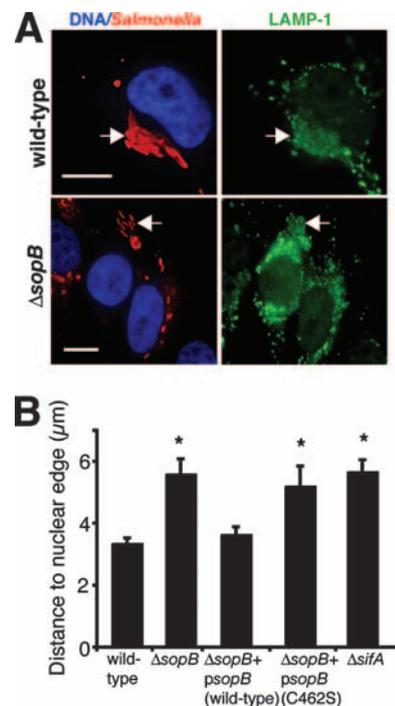

FIG. 6. SopB is required for maintaining SCV positioning in host cells during infection. (A) HeLa cells were infected with the indicated serovar Typhimurium strains for 10 h. *Salmonella* is shown in red, LAMP-1 is shown in green, and nuclei are shown in blue. Arrows indicate LAMP-1$^+$ bacteria. Bars, 10 μm. (B) Measurements of LAMP-1$^+$ bacteria to the closest nuclear edge. Averages ± SE are shown. *, significantly different from WT controls ($P < 0.05$), as determined by one-way ANOVA and Dunnett post hoc analysis.

that SopB acts independently of SifA to regulate SCV positioning.

Myosin II activation complements the SCV positioning defect of $\Delta sopB$ bacteria. Our studies suggest that SopB, by activating Rho family GTPases, mediates SCV positioning via myosin II activation. We hypothesized that activation of myosin II by pharmacologic or genetic means would complement positioning of the $\Delta sopB$ mutant SCV. HeLa cells were infected with $\Delta sopB$ bacteria in the presence or absence of calyculin A, a myosin II phosphatase inhibitor that maintains myosin activity (26). In control cells, $\Delta sopB$ mutant SCVs were 5.4 ± 0.3 μm from the nucleus at 8 h p.i. However, in the presence of calyculin A, they localized close to the nuclear edge (2.7 ± 0.3 μm) (Fig. 8A and B). Hence, inhibition of myosin II phosphatase activity (i.e., maintaining activation of myosin II) restored normal intracellular positioning of the $\Delta sopB$ mutant SCV. Similar results were obtained with $\Delta sopB$ bacterium-infected cells by prior transfection with constitutively active mutants of Rho GTPases (RhoA with the Q63L mutation [RhoA-Q63L], Cdc42 with the Q61L mutation [Cdc42-Q61L], and RhoG with the Q61L mutation [RhoG-Q61L]) (Fig. 8C and D). Furthermore, transfection of HeLa cells with a constitutively active MLC (36), CAT-ROCK, or SopB was sufficient to complement $\Delta sopB$ mutant positioning (Fig. 8E). The average cell surface areas of the various transfected cells were not significantly different from GFP-transfected controls, except for RhoA-Q63L-transfected cells,
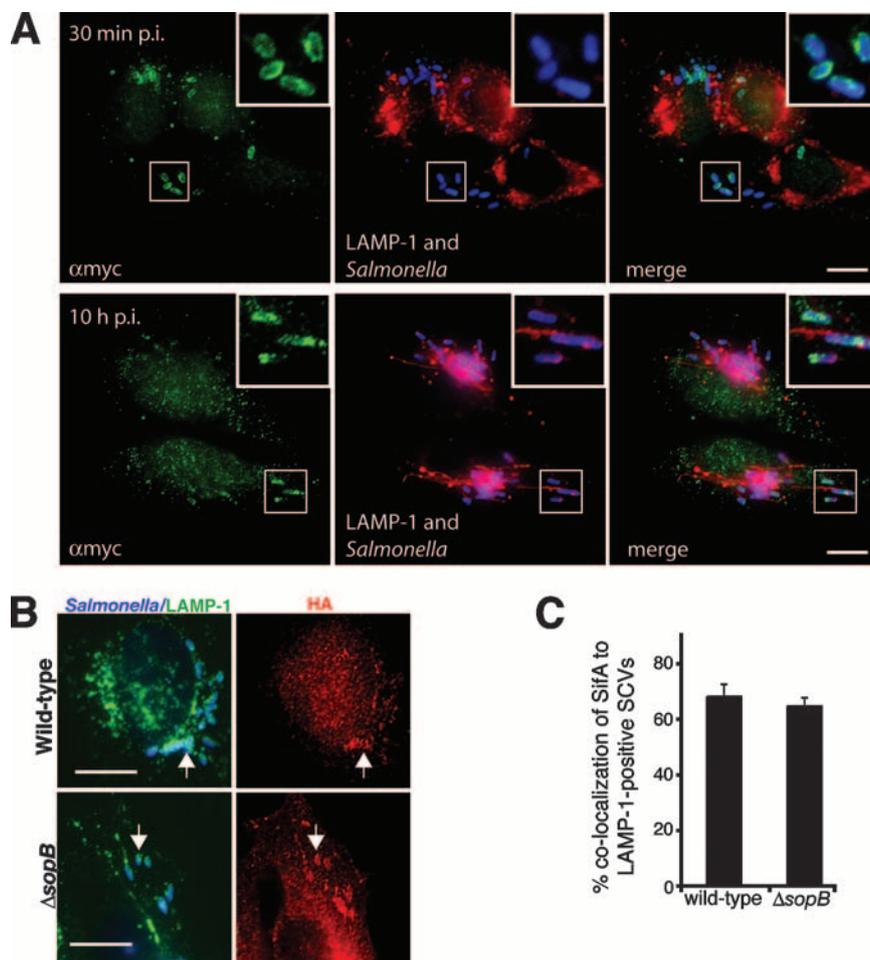
FIG. 7. SopB is localized to SCVs and does not affect SifA localization. (A) HeLa cells were infected with Δ*sopB* serovar Typhimurium (blue) expressing WT myc-tagged SopB (αmyc; green) for 30 min or 10 h. LAMP-1 is shown in red. (B) Cells were infected with WT serovar Typhimurium with p*sifA-2HA* or an isogenic Δ*sopB* strain with p*sifA-2HA* for 8 h. *Salmonella* is shown in blue, LAMP-1 is shown in green, and HA is shown in red. Arrows indicate LAMP-1$^+$ bacteria colocalizing with SifA. (C) Percentages of LAMP-1$^+$ bacteria in samples shown in panel B that colocalized with SifA (HA). Averages ± SE are shown. *, significantly different from WT ($P < 0.05$). Bars, 10 μm.

which were smaller than the controls (Fig. 8F). Overall, this shows that the capacity for normal SCV positioning can be restored to Δ*sopB* bacteria by activating myosin II, suggesting that myosin II acts downstream of SopB during serovar Typhimurium infection.

SopB is sufficient to activate myosin II. We infected HeLa cells with serovar Typhimurium for 2 h and immunoblotted infected cell extracts with an antibody specific for MLC phosphorylated at its two activation site residues, Ser18/Thr19 (PP-MLC). Infection with WT serovar Typhimurium did not lead to a global increase in PP-MLC in comparison to uninfected cells or cells infected with Δ*sopB* bacteria (data not shown). The majority of cellular myosin II remained associated with actin stress fibers during infection, and very little was detected on SCVs (Fig. 9A, top row). Therefore, global levels of PP-MLC would not be predicted to change during serovar Typhimurium infection. Interestingly, blebbistatin treatment allowed us to detect a significantly greater association of myosin II with both SCVs and Sifs (Fig. 9A, second and third rows, and B).

As an alternative strategy to determine if SopB is sufficient for myosin II activation (via phosphorylation of MLC), HeLa cells were transfected with SopB, RhoA-Q63L, Cdc42-Q61L, RhoG-Q61L, or GFP and immunostained for PP-MLC. Transfection of SopB resulted in the accumulation of PP-MLC on actin stress fibers, which was not observed for control GFP-transfected cells (Fig. 10A). Cells transfected with RhoA-Q63L showed the most robust PP-MLC staining, while SopB, Cdc42-Q61L, and RhoG-Q61L had intermediate effects (Fig. 10A and B). Cells transfected with SopB also demonstrated an increase in PP-MLC levels (similar to those of calyculin A-treated cells) compared to those of untreated controls and GFP-transfected controls (approximately 90% and 24% higher levels, respectively) according to Western blotting results (Fig. 10C). Overall, these results demonstrate that SopB expression is sufficient to mediate MLC phosphorylation and myosin II activation.

DISCUSSION

Recent studies have shown that positioning of the SCV near the nucleus is controlled, in part, by microtubule motors (1, 10, 29, 58). Here, we demonstrated that an actin-based motor,
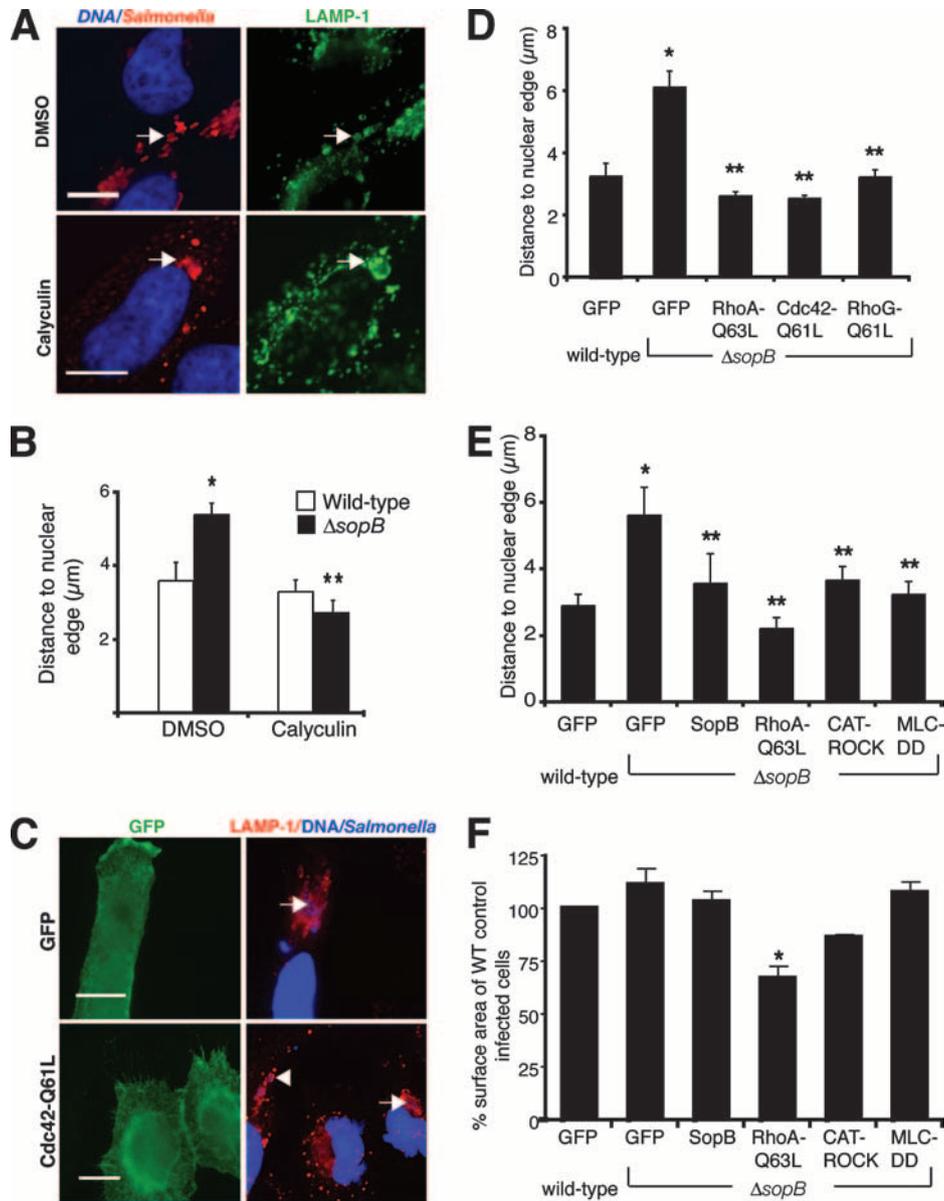
FIG. 8. SCV positioning of Δ*sopB* bacteria is complemented by inhibition of myosin II phosphatase or by expression of constitutively active Rho GTPases. (A) Positions of serovar Typhimurium bacteria (red) 8 h p.i. in HeLa cells treated with calyculin A or DMSO. LAMP-1 is shown in green, and nuclei are shown in blue. Arrows indicate LAMP-1^{+} bacteria. Bars, 10 μm. (B) Measurements of distances from LAMP-1^{+} bacteria to the closest nuclear edge in drug-treated cells. Averages ± SE are shown. *, significantly different from the respective DMSO-treated controls ($P <$ 0.05), as determined by a two-tailed, unpaired *t* test. (C) Positions of Δ*sopB* serovar Typhimurium bacteria (blue) 10 h p.i. in cells expressing GFP or Cdc42-Q61L (green). LAMP-1 is shown in red, and nuclei are shown in blue. Bacteria in transfected cells (arrows) and an untransfected cell (arrowhead) are indicated. Bars, 10 μm. (D) Measurements of distances from LAMP-1^{+} bacteria to the closest nuclear edge in transfected cells. Averages ± SE are shown. (E) Measurements of distances from LAMP-1^{+} bacteria to the closest nuclear edge in transfected cells. Averages ± SD are shown. (F) Comparison of average cell surface areas of transfected, infected cells to the average cell surface areas of control WT-infected cells expressing GFP. For panels D to F, asterisks indicate that the values are significantly different from those for the WT controls ($P <$ 0.05), and double asterisks indicate that the values are significantly different from the values for the respective GFP-expressing controls ($P <$ 0.05), as determined by one-way ANOVA and Dunnett post hoc analysis.

myosin II, also contributes to spatial control of SCVs. We demonstrated that, as with microtubule motor activity, myosin II activity is modulated by a type III secreted effector protein (SopB). Our studies reveal a previously unappreciated intersection of the microtubule and actin cytoskeletons that impact the SCV.

Myosin II, along with kinesin and dynein, contributes to a

remarkable balance of cytoskeletal motors acting on the SCV. Here, we demonstrated that myosin II counters the activity of PipB2, which recruits kinesin to the SCV (29). Also countering the activity of the PipB2/kinesin complex is SifA, which recruits the kinesin uncoupler SKIP to SCVs (10). SifA is recruited to the SCV by a SPI-1 effector, SipA, and cooperation between SifA and SipA is required for correct perinuclear positioning
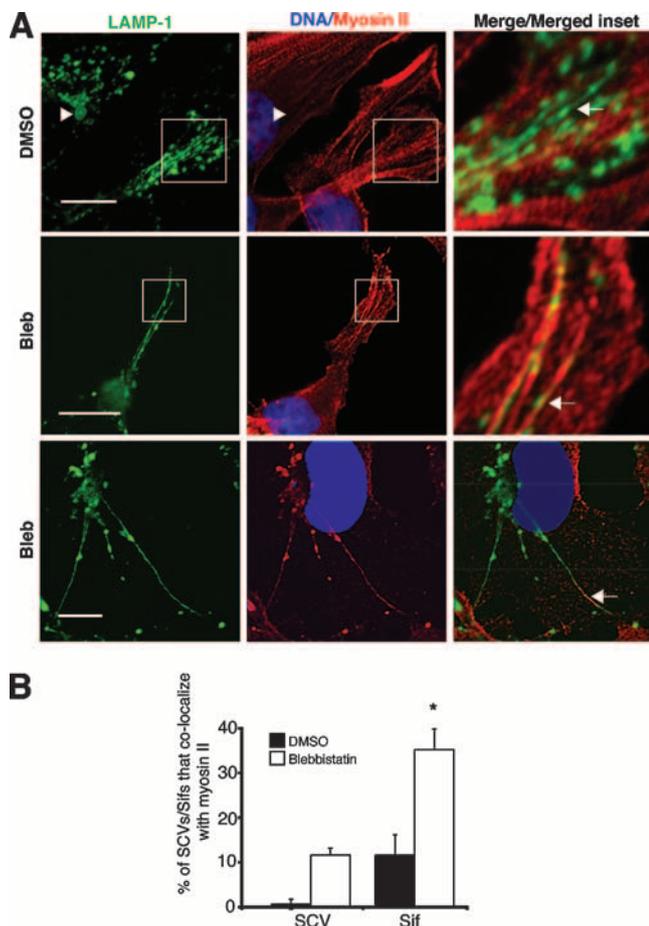
FIG. 9. Myosin II is present on SCVs and Sifs in blebbistatin-treated cells. (A) Colocalization of myosin II (red) with Sifs (LAMP-1; green) in serovar Typhimurium (DAPI; blue)-infected HeLa cells (8 h p.i.) is indicated by arrows. Arrowheads indicate that there was no colocalization. Cells were analyzed by immunofluorescence (top row) or confocal microscopy (middle and lower rows). Magnified boxed areas are shown in a merge. Bars, 10 μm. (B) For samples shown in panel A, SCVs/Sifs were scored for the presence or absence of myosin II. Averages ± SE are shown. *, significantly different from respective DMSO-treated controls ($P < 0.05$), as determined by a two-tailed, unpaired t test.

(11). Brawn et al. suggest that SipA, SifA, and SKIP might compose a multiprotein SCV regulatory complex (11). Deletion of *sifA* (15) or *sseF* and *sseG* (which recruit dynein) (1, 15) or inhibition of myosin II (this study) leads to centrifugal SCV displacement. Therefore, it would appear that the PipB2/kinesin complex provides a dominant centrifugal force on SCVs that requires multiple complementary forces to counter it and maintain the SCV near the nucleus. However, it should be noted that inhibiting myosin II led to centrifugal SCV displacement even without significant kinesin accumulation on SCVs (Fig. 4), suggesting that basal levels of kinesin are sufficient to mediate peripheral displacement of SCVs if given the opportunity.

The balance of cytoskeletal forces acting on the SCV must be finely balanced or else its integrity is disrupted (10, 25). Here, we showed that myosin II inhibition in HeLa cells leads to destabilization of the SCV and escape of bacteria into the

cytosol. The deacylase activity of SseJ was found to mediate the escape of bacteria when myosin II was inhibited. Similarly, SseJ mediates SCV destabilization in cells infected with Δ*sifA* bacteria (51, 60). Therefore, our studies reveal how serovar Typhimurium utilizes both actin- and microtubule-based motors to compensate for the membrane disrupting ability of SseJ to maintain the SCV.

The SPI-1 effector SopB is conserved in most contemporary serovars of *Salmonella*, suggesting that it has evolved as an essential component of their pathogenic repertoire (50, 57). Indeed, SopB has been shown to play a role in *Salmonella* pathogenesis in several animal models (50, 79). Furthermore, this effector has been linked to a remarkable number of cellular phenotypes associated with *Salmonella* infection, including invasion of nonphagocytic cells (5, 54, 56, 73, 80), early maturation of the SCV (34), modulation of ion channel activity (7), and induction of nitric oxide synthase (17). SopB is delivered into the host cell via the SPI-1 T3SS during invasion and persists in host cells for up to 12 h (17). The data presented here significantly expand the number of known host cell processes that can be affected by SopB and provide evidence for cross talk between effectors of the SPI-1 and SPI-2 T3SS. This evidence supports studies by Brawn et al. showing a functional relationship between the SPI-1 effector SipA and the SPI-2 effector SifA (11).

SopB is a phosphatase with a broad substrate specificity for inositol phosphates and phosphoinositides in vitro (34, 42, 50, 80). However, the in vivo substrates of SopB remain unclear (18), and it is not known how its phosphatase activity mediates Rho family GTPase activation. Data presented here suggest that SopB activates myosin II locally through a Rho/ROCK/MLC signaling pathway that leads to correct SCV positioning. Localized myosin II activity on an endosomal compartment has been observed in other systems. For example, Sturge et al. have reported that the Endo180 receptor can generate localized and sustained Rho/ROCK/MLC signaling during focal adhesion disassembly (71). Our studies also indicated that activated Cdc42 and RhoG led to intermediate levels of myosin II activation, as indicated by PP-MLC immunofluorescence (Fig. 10B). This would explain why positioning of the Δ*sopB* mutant SCVs could be complemented by the expression of these proteins (Fig. 8D). The mechanism(s) by which SopB can activate these small GTPases is presently unclear and would be interesting to investigate further.

Several reports (37, 53) have shown that marked apoptosis of *Salmonella*-infected epithelial cells occurs at time points (>12 h p.i.) later than those used in our studies (<10 h p.i.). Apoptosis of infected epithelial cells is delayed through the activation of Akt by SopB (38). Since we observed SCV positioning effects as early as 2 h p.i., it is therefore unlikely that changes in host cell morphology caused by *Salmonella*-induced apoptosis contributed to any differences noted in SCV localization. Knodler et al. noted that less than 10% of HeLa cells infected with a *sopB* mutant exhibited evidence of apoptosis at 4 h p.i., in comparison to WT-infected cells, which displayed approximately 5% apoptosis (38). It is possible that this slight difference may have affected mutant SCV localization; however, we observed no significant change in cell surface area between WT and *sopB*-infected HeLa cells even at 10 h p.i.

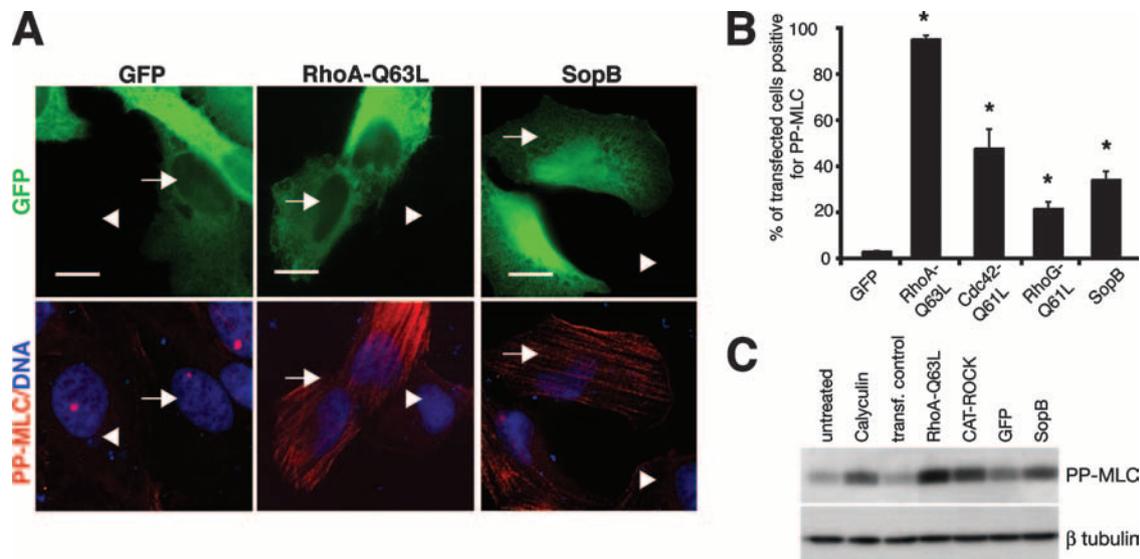Despite the obvious effect of myosin II on SCV stability and

FIG. 10. SopB expression is sufficient to induce myosin II phosphorylation and is required for activation of myosin II on Sifs. (A) PP-MLC (red) staining in HeLa cells expressing GFP, RhoA-Q63L, or SopB (green). Nuclei are shown in blue. Transfected cells are indicated by arrows, and nontransfected cells are indicated by arrowheads. (B) Percentage of transfected cells positive for PP-MLC staining. Averages ± SD are shown. *, significantly different from GFP-expressing controls ($P < 0.05$), as determined by one-way ANOVA and Dunnett post hoc analyses. (C) Western blot showing MLC phosphorylation in cells treated with calyculin A, expressing RhoA-Q63L, CAT-ROCK, GFP, or SopB, or mock transfected without DNA (transf. control).

positioning, we were unable to detect myosin II on SCVs by using immunofluorescence microscopy, and very little association with Sifs was observed (Fig. 9). We also could not detect the association of overexpressed monomeric red fluorescent protein-myosin IIA with SCVs/Sifs (data not shown). It is possible that myosin II associates transiently with SCVs/Sifs and that its steady-state levels on these compartments are not detectable with the methods used. Interestingly, blebbistatin treatment allowed us to detect significant levels of association of myosin II with both SCVs and Sifs (Fig. 9). It is possible that blebbistatin treatment traps myosin II on a fraction of SCVs/Sifs, preventing its release by blocking its ATPase activity. A similar trapping of microtubule motors on their respective cytoskeletal filaments/cargo using specific drugs or nonhydrolyzable ATP analogues has been reported (9, 14). The observation that myosin II can associate with SCVs/Sifs (albeit under artificial conditions) suggests that this motor acts locally at this compartment during infection. However, we cannot rule out the alternate possibility that myosin II is acting distally to the SCV to promote its positioning in host cells.

In summary, our data provide novel insight into how serovar Typhimurium maintains spatial control and stability of the SCV in host cells during infection. We have demonstrated a role for an actin-based motor in the regulation of SCV positioning, showing that microtubule motors are not the only host motor proteins involved in this process. We are beginning to understand the dynamic cytoskeletal forces that act upon the SCV during infection and how the bacteria control these forces to their benefit. Our study also reveals an unappreciated cross talk between effectors of the SPI-1 and SPI-2 T3SS. The finding that a SPI-1 effector (SopB) can impact SCV dynamics during late stages of infection (up to 10 h p.i. in this study)

suggests that effector activities are even more dynamically coordinated than previously thought.

REFERENCES

1. **Abrahams, G. L., P. Muller, and M. Hensel.** 2006. Functional dissection of SseF, a type III effector protein involved in positioning the *Salmonella*-containing vacuole. Traffic **7:**950–965.
2. **Amano, M., K. Chihara, N. Nakamura, T. Kaneko, Y. Matsuura, and K. Kaibuchi.** 1999. The COOH terminus of Rho-kinase negatively regulates Rho-kinase activity. J. Biol. Chem. **274:**32418–32424.
3. **Amano, M., M. Ito, K. Kimura, Y. Fukata, K. Chihara, T. Nakano, Y. Matsuura, and K. Kaibuchi.** 1996. Phosphorylation and activation of myosin by Rho-associated kinase (Rho-kinase). J. Biol. Chem. **271:**20246–20249.
4. **Araki, N., T. Hatae, A. Furukawa, and J. A. Swanson.** 2003. Phosphoinositide-3-kinase-independent contractile activities associated with Fcγ-receptor-mediated phagocytosis and macropinocytosis in macrophages. J. Cell Sci. **116:**247–257.
5. **Bakowski, M. A., J. T. Cirulis, N. F. Brown, B. B. Finlay, and J. H. Brumell.** 2007. SopD acts cooperatively with SopB during *Salmonella enterica* serovar Typhimurium invasion. Cell. Microbiol. **9:**2839–2855.

6. **Berg, J. S., B. C. Powell, and R. E. Cheney.** 2001. A millennial myosin census. Mol. Biol. Cell **12:**780–794.

7. **Bertelsen, L. S., G. Paesold, S. L. Marcus, B. B. Finlay, L. Eckmann, and K. E. Barrett.** 2004. Modulation of chloride secretory responses and barrier function of intestinal epithelial cells by the *Salmonella* effector protein SigD. Am. J. Physiol. Cell Physiol. **287:**C939–C948.

8. **Beuzón, C. R., S. P. Salcedo, and D. W. Holden.** 2002. Growth and killing of a *Salmonella enterica* serovar Typhimurium *sifA* mutant strain in the cytosol of different host cell lines. Microbiology **148:**2705–2715.

9. **Block, S. M., L. S. Goldstein, and B. J. Schnapp.** 1990. Bead movement by single kinesin molecules studied with optical tweezers. Nature **348:**348–352.

10. **Boucrot, E., T. Henry, J. P. Borg, J. P. Gorvel, and S. Meresse.** 2005. The intracellular fate of *Salmonella* depends on the recruitment of kinesin. Science **308:**1174–1178.

11. **Brawn, L. C., R. D. Hayward, and V. Koronakis.** 2007. *Salmonella* SPI1 effector SipA persists after entry and cooperates with a SPI2 effector to regulate phagosome maturation and intracellular replication. Cell Host Microbe **1:**63–75.

12. **Brumell, J. H., D. L. Goosney, and B. B. Finlay.** 2002. SifA, a type III secreted effector of *Salmonella typhimurium*, directs *Salmonella*-induced filament (Sif) formation along microtubules. Traffic **3:**407–415.

13. **Brumell, J. H., P. Tang, M. L. Zaharik, and B. B. Finlay.** 2002. Disruption of the *Salmonella*-containing vacuole leads to increased replication of *Salmonella enterica* serovar Typhimurium in the cytosol of epithelial cells. Infect. Immun. **70:**3264–3270.

14. **Chua, P. R., D. M. Roof, Y. Lee, R. Sakowicz, D. Clarke, D. Pierce, T. Stephens, M. Hamilton, B. Morgan, D. Morgans, T. Nakai, A. Tomasi, and M. E. Maxon.** 2007. Effective killing of the human pathogen *Candida albicans* by a specific inhibitor of non-essential mitotic kinesin Kip1p. Mol. Microbiol. **65:**347–362.

15. **Deiwick, J., S. P. Salcedo, E. Boucrot, S. M. Gilliland, T. Henry, N. Petermann, S. R. Waterman, J. P. Gorvel, D. W. Holden, and S. Meresse.** 2006. The translocated *Salmonella* effector proteins SseF and SseG interact and are required to establish an intracellular replication niche. Infect. Immun. **74:**6965–6972.

16. **Diakonova, M., G. Bokoch, and J. A. Swanson.** 2002. Dynamics of cytoskeletal proteins during Fcγ receptor-mediated phagocytosis in macrophages. Mol. Biol. Cell **13:**402–411.

17. **Drecktrah, D., L. A. Knodler, K. Galbraith, and O. Steele-Mortimer.** 2005. The *Salmonella* SPI1 effector SopB stimulates nitric oxide production long after invasion. Cell. Microbiol. **7:**105–113.

18. **Drecktrah, D., L. A. Knodler, and O. Steele-Mortimer.** 2004. Modulation and utilization of host cell phosphoinositides by *Salmonella* spp. Infect. Immun. **72:**4331–4335.

19. **Durán, J. M., F. Valderrama, S. Castel, J. Magdalena, M. Tomas, H. Hosoya, J. Renau-Piqueras, V. Malhotra, and G. Egea.** 2003. Myosin motors and not actin comets are mediators of the actin-based Golgi-to-endoplasmic reticulum protein transport. Mol. Biol. Cell **14:**445–459.

20. **Fields, P. I., R. V. Swanson, C. G. Haidaris, and F. Heffron.** 1986. Mutants of *Salmonella typhimurium* that cannot survive within the macrophage are avirulent. Proc. Natl. Acad. Sci. USA **83:**5189–5193.

21. **Finlay, B. B., S. Ruschkowski, and S. Dedhar.** 1991. Cytoskeletal rearrangements accompanying salmonella entry into epithelial cells. J. Cell Sci. **99:**283–296.

22. **Galán, J. E., and R. Curtiss III.** 1989. Cloning and molecular characterization of genes whose products allow *Salmonella typhimurium* to penetrate tissue culture cells. Proc. Natl. Acad. Sci. USA **86:**6383–6387.

23. **Galan, J. E., and D. Zhou.** 2000. Striking a balance: modulation of the actin cytoskeleton by *Salmonella*. Proc. Natl. Acad. Sci. USA **97:**8754–8761.

24. **Garcia-del Portillo, F., M. B. Zwick, K. Y. Leung, and B. B. Finlay.** 1993. *Salmonella* induces the formation of filamentous structures containing lysosomal membrane glycoproteins in epithelial cells. Proc. Natl. Acad. Sci. USA **90:**10544–10548.

25. **Guignot, J., E. Caron, C. Beuzon, C. Bucci, J. Kagan, C. Roy, and D. W. Holden.** 2004. Microtubule motors control membrane dynamics of *Salmonella*-containing vacuoles. J. Cell Sci. **117:**1033–1045.

26. **Gupton, S. L., and C. M. Waterman-Storer.** 2006. Spatiotemporal feedback between actomyosin and focal-adhesion systems optimizes rapid cell migration. Cell **125:**1361–1374.

27. **Hardt, W. D., L. M. Chen, K. E. Schuebel, X. R. Bustelo, and J. E. Galan.** 1998. *S. typhimurium* encodes an activator of Rho GTPases that induces membrane ruffling and nuclear responses in host cells. Cell **93:**815–826.

28. **Harrison, R. E., J. H. Brumell, A. Khandani, C. Bucci, C. C. Scott, X. Jiang, B. B. Finlay, and S. Grinstein.** 2004. *Salmonella* impairs RILP recruitment to Rab7 during maturation of invasion vacuoles. Mol. Biol. Cell **15:**3146–3154.

29. **Henry, T., C. Couillault, P. Rockenfeller, E. Boucrot, A. Dumont, N. Schroeder, A. Hermant, L. A. Knodler, P. Lecine, O. Steele-Mortimer, J. P. Borg, J. P. Gorvel, and S. Meresse.** 2006. The *Salmonella* effector protein PipB2 is a linker for kinesin-1. Proc. Natl. Acad. Sci. USA **103:**13497–13502.

30. **Hensel, M.** 2000. *Salmonella* pathogenicity island 2. Mol. Microbiol. **36:**1015–1023.

31. **Hensel, M., J. E. Shea, B. Raupach, D. Monack, S. Falkow, C. Gleeson, T. Kubo, and D. W. Holden.** 1997. Functional analysis of *ssaJ* and the *ssaK/U* operon, 13 genes encoding components of the type III secretion apparatus of *Salmonella* pathogenicity island 2. Mol. Microbiol. **24:**155–167.

32. **Hensel, M., J. E. Shea, S. R. Waterman, R. Mundy, T. Nikolaus, G. Banks, A. Vazquez-Torres, C. Gleeson, F. C. Fang, and D. W. Holden.** 1998. Genes encoding putative effector proteins of the type III secretion system of *Salmonella* pathogenicity island 2 are required for bacterial virulence and proliferation in macrophages. Mol. Microbiol. **30:**163–174.

33. **Heo, W. D., T. Inoue, W. S. Park, M. L. Kim, B. O. Park, T. J. Wandless, and T. Meyer.** 2006. PI(3,4,5)P3 and PI(4,5)P2 lipids target proteins with polybasic clusters to the plasma membrane. Science **314:**1458–1461.

34. **Hernandez, L. D., K. Hueffer, M. R. Wenk, and J. E. Galan.** 2004. *Salmonella* modulates vesicular traffic by altering phosphoinositide metabolism. Science **304:**1805–1807.

35. **Hoiseth, S. K., and B. A. Stocker.** 1981. Aromatic-dependent *Salmonella typhimurium* are non-virulent and effective as live vaccines. Nature **291:**238–239.

36. **Iwasaki, T., M. Murata-Hori, S. Ishitobi, and H. Hosoya.** 2001. Diphosphorylated MRLC is required for organization of stress fibers in interphase cells and the contractile ring in dividing cells. Cell Struct. Funct. **26:**677–683.

37. **Kim, J. M., L. Eckmann, T. C. Savidge, D. C. Lowe, T. Witthoft, and M. F. Kagnoff.** 1998. Apoptosis of human intestinal epithelial cells after bacterial invasion. J. Clin. Investig. **102:**1815–1823.

38. **Knodler, L. A., B. B. Finlay, and O. Steele-Mortimer.** 2005. The *Salmonella* effector protein SopB protects epithelial cells from apoptosis by sustained activation of Akt. J. Biol. Chem. **280:**9058–9064.

39. **Kubori, T., and J. E. Galan.** 2003. Temporal regulation of salmonella virulence effector function by proteasome-dependent protein degradation. Cell **115:**333–342.

40. **Lehmann, M. J., N. M. Sherer, C. B. Marks, M. Pypaert, and W. Mothes.** 2005. Actin- and myosin-driven movement of viruses along filopodia precedes their entry into cells. J. Cell Biol. **170:**317–325.

41. **Lutz, G. J., and R. L. Lieber.** 1999. Skeletal muscle myosin II structure and function. Exerc. Sport Sci. Rev. **27:**63–77.

42. **Marcus, S. L., L. A. Knodler, and B. B. Finlay.** 2002. *Salmonella enterica* serovar Typhimurium effector SigD/SopB is membrane-associated and ubiquitinated inside host cells. Cell. Microbiol. **4:**435–446.

43. **Marcus, S. L., M. R. Wenk, O. Steele-Mortimer, and B. B. Finlay.** 2001. A synaptojanin-homologous region of *Salmonella typhimurium* SigD is essential for inositol phosphatase activity and Akt activation. FEBS Lett. **494:**201–207.

44. **Masszi, A., C. Di Ciano, G. Sirokmany, W. T. Arthur, O. D. Rotstein, J. Wang, C. A. McCulloch, L. Rosivall, I. Mucsi, and A. Kapus.** 2003. Central role for Rho in TGF-beta1-induced alpha-smooth muscle actin expression during epithelial-mesenchymal transition. Am. J. Physiol. Renal Physiol. **284:**F911–F924.

45. **Matsumura, F.** 2005. Regulation of myosin II during cytokinesis in higher eukaryotes. Trends Cell Biol. **15:**371–377.

46. **Méresse, S., K. E. Unsworth, A. Habermann, G. Griffiths, F. Fang, M. J. Martinez-Lorenzo, S. R. Waterman, J. P. Gorvel, and D. W. Holden.** 2001. Remodelling of the actin cytoskeleton is essential for replication of intravacuolar *Salmonella*. Cell. Microbiol. **3:**567–577.

47. **Mermall, V., P. L. Post, and M. S. Mooseker.** 1998. Unconventional myosins in cell movement, membrane traffic, and signal transduction. Science **279:**527–533.

48. **Miao, E. A., M. Brittnacher, A. Haraga, R. L. Jeng, M. D. Welch, and S. I. Miller.** 2003. *Salmonella* effectors translocated across the vacuolar membrane interact with the actin cytoskeleton. Mol. Microbiol. **48:**401–415.

49. **Miao, E. A., C. A. Scherer, R. M. Tsolis, R. A. Kingsley, L. G. Adams, A. J. Baumler, and S. I. Miller.** 1999. *Salmonella typhimurium* leucine-rich repeat proteins are targeted to the SPI1 and SPI2 type III secretion systems. Mol. Microbiol. **34:**850–864.

50. **Norris, F. A., M. P. Wilson, T. S. Wallis, E. E. Galyov, and P. W. Majerus.** 1998. SopB, a protein required for virulence of *Salmonella dublin*, is an inositol phosphate phosphatase. Proc. Natl. Acad. Sci. USA **95:**14057–14059.

51. **Ohlson, M. B., K. Fluhr, C. L. Birmingham, J. H. Brumell, and S. I. Miller.** 2005. SseJ deacylase activity by *Salmonella enterica* serovar Typhimurium promotes virulence in mice. Infect. Immun. **73:**6249–6259.

52. **Olazabal, I. M., E. Caron, R. C. May, K. Schilling, D. A. Knecht, and L. M. Machesky.** 2002. Rho-kinase and myosin-II control phagocytic cup formation during CR, but not FcγR, phagocytosis. Curr. Biol. **12:**1413–1418.

53. **Paesold, G., D. G. Guiney, L. Eckmann, and M. F. Kagnoff.** 2002. Genes in the *Salmonella* pathogenicity island 2 and the *Salmonella* virulence plasmid are essential for *Salmonella*-induced apoptosis in intestinal epithelial cells. Cell. Microbiol. **4:**771–781.

54. **Patel, J. C., and J. E. Galan.** 2006. Differential activation and function of Rho GTPases during *Salmonella*-host cell interactions. J. Cell Biol. **175:**453–463.

55. **Poh, J., C. Odendall, A. Spanos, C. Boyle, M. Liu, P. Freemont, and D. W. Holden.** 2008. SteC is a *Salmonella* kinase required for SPI-2-dependent F-actin remodelling. Cell. Microbiol. **10:**20–30.

56. **Raffatellu, M., R. P. Wilson, D. Chessa, H. Andrews-Polymenis, Q. T. Tran,**

S. Lawhon, S. Khare, L. G. Adams, and A. J. Baumler. 2005. SipA, SopA, SopB, SopD, and SopE2 contribute to *Salmonella enterica* serotype Typhimurium invasion of epithelial cells. Infect. Immun. **73:**146–154.

57. **Rahman, H.** 2006. Prevalence & phenotypic expression of *sopB* gene among clinical isolates of *Salmonella enterica*. Indian J. Med. Res. **123:**83–88.

58. **Ramsden, A. E., L. J. Mota, S. Munter, S. L. Shorte, and D. W. Holden.** 2007. The SPI-2 type III secretion system restricts motility of *Salmonella*-containing vacuoles. Cell. Microbiol. **9:**2517–2529.

59. **Rathman, M., P. de Lanerolle, H. Ohayon, P. Gounon, and P. Sansonetti.** 2000. Myosin light chain kinase plays an essential role in *S. flexneri* dissemination. J. Cell Sci. **113:**3375–3386.

60. **Ruiz-Albert, J., X. J. Yu, C. R. Beuzon, A. N. Blakey, E. E. Galyov, and D. W. Holden.** 2002. Complementary activities of SseJ and SifA regulate dynamics of the *Salmonella typhimurium* vacuolar membrane. Mol. Microbiol. **44:**645–661.

61. **Salcedo, S. P., and D. W. Holden.** 2003. SseG, a virulence protein that targets *Salmonella* to the Golgi network. EMBO J. **22:**5003–5014.

62. **Schlumberger, M. C., and W. D. Hardt.** 2006. *Salmonella* type III secretion effectors: pulling the host cell's strings. Curr. Opin. Microbiol. **9:**46–54.

63. **Shea, J. E., M. Hensel, C. Gleeson, and D. W. Holden.** 1996. Identification of a virulence locus encoding a second type III secretion system in *Salmonella typhimurium*. Proc. Natl. Acad. Sci. USA **93:**2593–2597.

64. **Smith, A. C., J. T. Cirulis, J. E. Casanova, M. A. Scidmore, and J. H. Brumell.** 2005. Interaction of the *Salmonella*-containing vacuole with the endocytic recycling system. J. Biol. Chem. **280:**24634–24641.

65. **Smith, A. C., W. D. Heo, V. Braun, X. Jiang, C. Macrae, J. E. Casanova, M. A. Scidmore, S. Grinstein, T. Meyer, and J. H. Brumell.** 2007. A network of Rab GTPases controls phagosome maturation and is modulated by *Salmonella enterica* serovar Typhimurium. J. Cell Biol. **176:**263–268.

66. **Sousa, S., D. Cabanes, A. El-Amraoui, C. Petit, M. Lecuit, and P. Cossart.** 2004. Unconventional myosin VIIa and vezatin, two proteins crucial for *Listeria* entry into epithelial cells. J. Cell Sci. **117:**2121–2130.

67. **Steele-Mortimer, O., J. H. Brumell, L. A. Knodler, S. Meresse, A. Lopez, and B. B. Finlay.** 2002. The invasion-associated type III secretion system of *Salmonella enterica* serovar Typhimurium is necessary for intracellular proliferation and vacuole biogenesis in epithelial cells. Cell. Microbiol. **4:**43–54.

68. **Steele-Mortimer, O., L. A. Knodler, S. L. Marcus, M. P. Scheid, B. Goh, C. G. Pfeifer, V. Duronio, and B. B. Finlay.** 2000. Activation of Akt/protein kinase B in epithelial cells by the *Salmonella typhimurium* effector *sigD*. J. Biol. Chem. **275:**37718–37724.

69. **Steele-Mortimer, O., S. Meresse, J. P. Gorvel, B. H. Toh, and B. B. Finlay.** 1999. Biogenesis of *Salmonella typhimurium*-containing vacuoles in epithelial cells involves interactions with the early endocytic pathway. Cell. Microbiol. **1:**33–49.

70. **Stender, S., A. Friebel, S. Linder, M. Rohde, S. Mirold, and W. D. Hardt.** 2000. Identification of SopE2 from *Salmonella typhimurium*, a conserved guanine nucleotide exchange factor for Cdc42 of the host cell. Mol. Microbiol. **36:**1206–1221.

71. **Sturge, J., D. Wienke, and C. M. Isacke.** 2006. Endosomes generate localized Rho-ROCK-MLC2-based contractile signals via Endo180 to promote adhesion disassembly. J. Cell Biol. **175:**337–347.

72. **Swanson, J. A., M. T. Johnson, K. Beningo, P. Post, M. Mooseker, and N. Araki.** 1999. A contractile activity that closes phagosomes in macrophages. J. Cell Sci. **112:**307–316.

73. **Terebiznik, M. R., O. V. Vieira, S. L. Marcus, A. Slade, C. M. Yip, W. S. Trimble, T. Meyer, B. B. Finlay, and S. Grinstein.** 2002. Elimination of host cell PtdIns(4,5)P(2) by bacterial SigD promotes membrane fission during invasion by *Salmonella*. Nat. Cell Biol. **4:**766–773.

74. **Tsolis, R. M., R. A. Kingsley, S. M. Townsend, T. A. Ficht, L. G. Adams, and A. J. Baumler.** 1999. Of mice, calves, and men. Comparison of the mouse typhoid model with other *Salmonella* infections. Adv. Exp. Med. Biol. **473:**261–274.

75. **Ueda, K., M. Murata-Hori, M. Tatsuka, and H. Hosoya.** 2002. Rho-kinase contributes to diphosphorylation of myosin II regulatory light chain in nonmuscle cells. Oncogene **21:**5852–5860.

76. **Unsworth, K. E., M. Way, M. McNiven, L. Machesky, and D. W. Holden.** 2004. Analysis of the mechanisms of *Salmonella*-induced actin assembly during invasion of host cells and intracellular replication. Cell. Microbiol. **6:**1041–1055.

77. **Wei, Q., and R. S. Adelstein.** 2000. Conditional expression of a truncated fragment of nonmuscle myosin II-A alters cell shape but not cytokinesis in HeLa cells. Mol. Biol. Cell **11:**3617–3627.

78. **Wilkinson, S., H. F. Paterson, and C. J. Marshall.** 2005. Cdc42-MRCK and Rho-ROCK signalling cooperate in myosin phosphorylation and cell invasion. Nat. Cell Biol. **7:**255–261.

79. **Zhang, S., R. L. Santos, R. M. Tsolis, S. Stender, W. D. Hardt, A. J. Baumler, and L. G. Adams.** 2002. The *Salmonella enterica* serotype Typhimurium effector proteins SipA, SopA, SopB, SopD, and SopE2 act in concert to induce diarrhea in calves. Infect. Immun. **70:**3843–3855.

80. **Zhou, D., L. M. Chen, L. Hernandez, S. B. Shears, and J. E. Galan.** 2001. A *Salmonella* inositol polyphosphatase acts in conjunction with other bacterial effectors to promote host cell actin cytoskeleton rearrangements and bacterial internalization. Mol. Microbiol. **39:**248–259.